Journal of Engineering Science and Technology Review 12 (3) (2019) 172 - 180

Research Article

JOURNAL OF
Engineering Science and Technology Review

www.jestr.org

Experimental Study of Mechanical Properties of Coarse-grained High Embankment Fillers

Feng Zhao[1], Maolong Zhao[2], Yanqing Zhang[3,*] and Chongchong Qi[4]

[1] *Ankang Highway Administration Bureau, Ankang, Shaanxi 725000, China*
[2] *Shaanxi Highway Construction Group Co., Ltd, Xi'an, Shaanxi 710068, China*
[3] *Xi'an University of Science and Technology, Xi'an, Shaanxi 710054, China*
[4] *School of Civil, Environmental and Mining Engineering, University of Western Australia, Perth, 6009, Australia*

Received 11 April 2019; Accepted 25 June 2019

Abstract

Mechanical properties of coarse-grained high embankment fillers are key factors that affect embankment stability. A large-scale triaxial shear tester is used to carry out consolidated drained and undrained shear tests on high embankment fillers. The mechanical properties and the stability of the high embankment in the filling process and operational period are analyzed under the background of a high rockfill embankment project (50.6 m filling height) located in the Qinba Mountain Area. Stress-strain characteristics and strength characteristics of fillers are analyzed and pore pressure coefficient was introduced to analyze filler deformation characteristics. The effects of grain breakage on filler strength and deformation are also discussed and the applicability of Duncan-Chang Model verified. Test results indicate the sample experience strain softening phenomenon under high confining pressure. Grain breakage index B_r is used to analyze the filler grain breakage features and the causes for this phenomenon are expounded. The degree of grain breakage increases significantly with confining pressure. Changes in the peak and critical-state friction angles of the fillers are related closely to grain breakage process. Under serious grain breakage, the friction angles decline significantly with grain breakage index. In the end, the applicability of Duncan-Chang model is analyzed on the test basis; neither the E~μ nor the E~B model can describe the deformation characteristics of coarse-grained embankment fillers very well. The results obtained in this study can provide a reference for the deformation characteristics of coarse-grained high embankment fillers and embankment stability analysis.

Keywords: High embankment; Coarse-grained fillers; Deformation; Grain breakage; Large-scale triaxial shear test; Duncan-Chang model

1. Introduction

With the increase in the construction of mountain highways, high embankments have endlessly come into being. In the construction of high embankments, coarse grains with large grain sizes are used mainly as fillers, the mechanical properties of which are of great importance to embankment stability. Coarse-grained embankment fillers refer to cohesionless mixtures composed of coarse grains such as rock blocks, detritus (or gravel and pebbles), aggregate chips, and stone powders or composite soil containing a large number of coarse grains in the cohesive soil. Coarse-grained materials are widespread in nature with large reserves and favorable engineering characteristics, such as easy compaction, strong water permeability, high strength, and uneasy liquidation under seismic load, and thus, they have been applied extensively to dam, highway, railway, airport and other projects [1].

Research emphasis and focus have been given to the stress-strain analysis of geotechnical building and stress-strain relation of coarse grains because of the construction of high embankments, high earth and rockfill dams, and high-rise buildings and the need to adapt to its requirements. The study of strength characteristics of coarse-grained soil has also moved from the general plane problem to a high-pressure state and complicated stress state. Grain size of coarse grains is large with complicated deformation mechanism, and strain softening characteristics, dilatancy, and grain breakage characteristics are considered in deformation and strength analysis.

Strain softening and strain hardening are two of the most common stress-stain relations of coarse-grained materials, which are related to test confining pressure and sample compactness. In the tri-axial shear test, coarse-grained soil presents low-pressure softening and high-pressure hardening under general circumstances. Establishing a constitutive model that considers the strain softening features on the test basis is a hotspot in the engineering circles and certain achievements have been obtained [2-3]. However, the model difference is large and the ranges of application are also different.

Dilatancy is a basic mechanical property of grain materials and an important feature different from other materials. Under the shear force, the grain position is changed, which causes volume change. Soil dilatancy has a great effect on soil strength. Many scholars have investigated soil dilatancy and established dilatancy theories [4-6]. However, the present dilatancy theories are established for sandy soil. These dilatancy theories have also been considered to be applicable to coarse-grained soil, but

*E-mail address: zhangyq@xust.edu.cn
ISSN: 1791-2377
doi:10.25103/jestr.123.23

with an increasing cognition of coarse-grained soil, it has been determined that coarse-grained soil can be crushed easily under high pressure. The dilatancy theories considering grain breakage need to be studied further.

According to classical soil mechanics, soil grains are incompressible and cannot be broken. Soil deformation is caused by pore compression inside the soil mass, water drainage, and grain reconstruction. However, soil grains especially coarse-grained soil, will experience partial or complete breakage under the stress effect of their own strength and grain breakage leads to changes in grading and compactness of coarse-grained soil, which affects soil deformation and strength. As coarse-grained soil has large grain size and is angular, and thus, it can easily go through grain breakage under the pressure action. Previous studies on coarse-grained soil are still in the exploratory phase, and its strength and deformation features have not been mastered completely and filling construction and quality inspection of coarse-grained fillers rely mainly on engineering experience.

A set of large-scale triaxial shear tests of coarse-grained high embankment fillers were carried out with the aim of providing test basis for understanding the mechanical properties of coarse-grained fillers and providing a reference for the stability analysis of National Highway 316 project in China and other similar projects.

2. State of the art

As a commonly used high embankment filling, coarse-grained soil has good compactness, high strength, and strong water permeability. However, as coarse-grained soils have great physical morphological differences and complicated deformation under the load effect, the present studies on coarse-grained embankment fillers are still in a preliminary stage. Numerous domestic and foreign scholars have investigated the characteristics of coarse-grained fillers. Lenart et al. [7] conducted a large-scale tri-axial experimental study of strength and deformation of sand-gravel materials, but the test confining pressure was low. Zhu et al. [8] carried out a large-scale triaxial humidifying deformation test and analyzed the change laws of volumetric and shear strains of coarse-grained humidifying body of slate with confining pressure and stress level without considering the material deformation and strength before humidification. Liu et al. [9] established a microstructure-based coarse-grained elastic-plastic constitutive model within the classical elastic-plastic theoretical framework and constructed hardening parameters that could realize a uniform description of dilatancy characteristics of coarse-grained material; however, when the material grading changed, the model was no longer applicable. Based on the fractal theory, Zhao et al. [10] studied the grading scaling method of coarse-grained materials, but this was not applicable in the circumstances with high content of fine grains. By considering the grading change caused by grain breakage, Sun et al. [11] studied the yield function of coarse-grained materials but did not consider the situation with high confining pressure. Yang et al. [12] conducted a numerical simulation study of grain breakage of coarse-grained materials but did not consider the complicated grain shape.

Some scholars have studied the deformation and strength characteristics of coarse-grained soil through experiments and numerical simulation without considering the effects of grain breakage. Khalkhali et al. [13] used the direct shear test and discrete element simulation to investigate the effects of grain size on mechanical behaviors of coarse-grained soil. Through a large-scale true triaxial equal proportion loading test under isobaric consolidation of coarse-grained materials in all directions, Jiang et al. [14] investigated the strength characteristic of coarse-grained materials under different intermediate principal stress coefficients. Tutumluer et al. [15] built a model to analyze the appearance features of coarse grains based on the three-view reconstruction method and conducted discrete element simulation of grains with different geometrical features. Based on the bi-mirror 3D imaging, Bian et al. [16] studied geometrical features of coarse-grained materials. Dorostkar et al. [17] used the discrete element method to study micromechanical characteristics of coarse-grained materials. Zhao et al. [18] investigated microstructure, compressibility, and strength of unsaturated coarse-grained materials. Meng et al. [19] carried out a large-scale tri-axial shear test and studied the deformation characteristics of coarse-grained materials under different grading conditions. Shi et al. [20] studied the strength and deformation characteristics of coarse-grained materials through the true tri-axial test. Fu et al. [21] explored the strength characteristics of coarse-grained materials under different pores and sizes through the direct shear test.

In this study, large-scale triaxial consolidated drained shear tests and consolidated undrained shear tests of coarse saturated argillaceous limestone samples were carried out to obtain deeper understanding of the mechanical characteristics of deformation property of coarse-grained embankment fillers and provide a reference for stability and settlement deformation analysis of the National Highway 316 project in China and other similar projects.

The remainder of this study is organized as follows: Section Three expounds on the test conditions; Section Four analyzes the test results of coarse-grained fillers such as stress-strain, deformation, strength, and grain breakage characteristics; Section Five analyses the applicability of Duncan-Chang model to coarse-grained fillers; and Section Six provides the summary and related conclusions of this study.

3. Methodology

3.1 Test equipment and test materials

This test was carried out on a large static triaxial apparatus (Fig. 1) from Nanjing Hydraulic Research Institute. The sample size was φ300 mm×700 mm and maximum limit of the grain size was 60 mm.

The test material was embankment filling of the reconstruction project of the Xunyang-Ankang Secondary Highway segment of the National Highway 316 in China. The material is composed of argillaceous limestone, with a rock softening coefficient of 0.73 and Type II rock quality level, and thus can be classified as hard rock difficult to soften. Basic properties of the sample can be seen in Tab. 1 and the grading curve is shown in Fig. 2.

Table 1. Indices of basic properties of sample

Test material	Specific gravity	Porosity	Test dry density (g/cm^3)	Saturated uniaxial compressive strength (MPa)
Argillaceous limestone	2.80	18.0%	2.30	46.5

Fig. 1. Large static triaxial apparatus

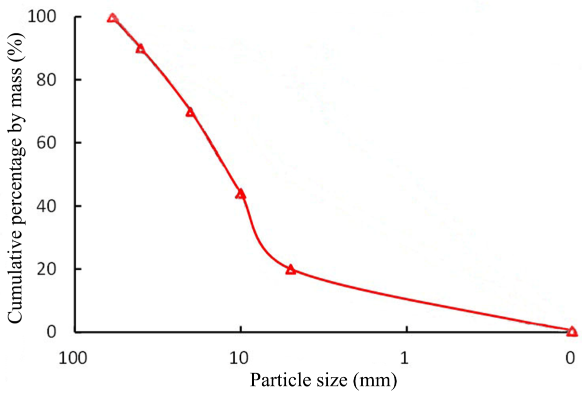

Fig. 2. Grading curve of embankment filler used in the test

3.2 Testing program

The required sample was calculated according to test requirements and was weighed in five equal portions by five grain size grades: 60–40 mm, 40–20 mm, 20–10 mm, 10–5 mm, and 5–0 mm. A porous plate was placed at the sample bottom, a rubber membrane was strapped on the pedestal, a forming barrel was installed, then the rubber membrane was coated on the outer wall of forming barrel, and air was exhausted so that rubber membrane clung to the inner wall of forming barrel. The first-layer sample was encased, the surface flattened, and the sample compacted using a vibrator. After the sample was well placed, the porous plate and sample cap were installed, rubber membrane tightened, the forming barrel removed (the sample after the removal of the forming barrel can be seen in Fig. 3), the pressure chamber installed and the gas vent opened. After the pressure chamber was filled with water, the gas vent was closed. The sample was saturated using the dripping saturation method. Then, the saturated sample was applied with confining pressure as required and then consolidated. After consolidation, the shear test was conducted until the sample failure or 15% of the axial strain of the sample was reached. The above process was repeated and the test carried out under confining pressures 200 kPa, 400 kPa, 600 kPa, and 800 kPa, respectively. The entire test was conducted in accordance with Geo-technical Testing Regulations (SL237 —1999), and the sample after shear test can be seen in Fig. 4.

Fig. 3. Completed sample

Fig. 4. Completed shear test

4. Result Analysis and Discussion

4.1 Stress-strain characteristic analysis

Fig. 5 shows the change curves of the generalized shear stress ratio (q/p) for the sample with axial strain (ε_1) in the consolidated drained test.

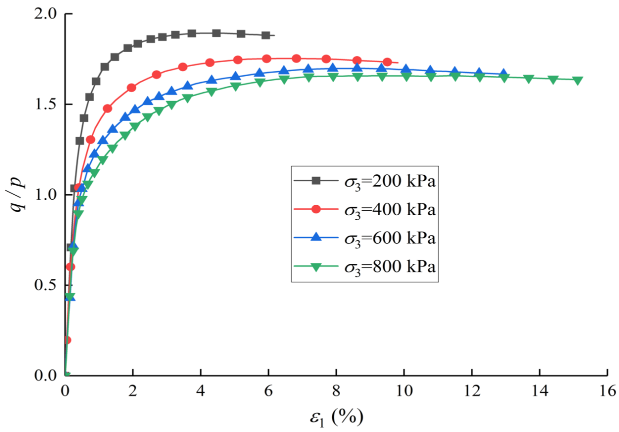

Fig. 5 Relation curves between generalized shear stress ratio-axial strain of the sample under drained condition

At the initial loading phase, the curves presented a linear growth trend and initial slopes of the curves were quite loose under different confining pressures. Both peak stress ratio and final generalized shear stress ratio of the curves declined as the confining pressure increased. Under four confining pressures, generalized shear stress ratio curve of the specimen presented weak strain softening with peak value. Under general circumstances, both fine-grained and coarse-grained soil will experience strain softening phenomenon under low confining pressure and strain hardening phenomenon under high confining pressure in the tri-axial shear test. In this study, the coarse-grained argillaceous limestone filler went through strain softening phenomenon under high confining pressure mainly because grains in the sample were broken and then its strength declined after peak stress was reached under high confining pressure.

The effect of grain breakage on filler strength was explained by sieving the sample before and after the test and using the grain breakage index B_r proposed by Hardin [22] to quantify the degree of grain breakage of the sample. B_r is defined as ratio of the difference between the areas confined by the grain size distribution curve and vertical line (grain size: 0.074 mm) before and after the test to the area combined by the grain size distribution curve before the test and 0.074 mm vertical line in the coordinate system. The x-coordinate is lg*d*, where d is the grain size and the y-coordinate is the percentage content exceeding a grain size. The results are shown in Fig. 11.

According to Fig. 11, the grain breakage of the specimen in the consolidated drained sheer test increased with confining pressure at high rate. Related studies [23-25] have reported that grain breakage is smaller under low confining pressure and that the increase in grain breakage will significantly degrade material strength. Using the tri-axial test of coarse-grained materials, Qin et al. [26] found an increase in confining pressure led to an increase in grain breakage. When breakage reached 0.21, an obvious decline in material strength was observed. The analysis showed that the sample experienced weak strain softening phenomenon under high confining pressure in the consolidated drained test, mainly because grain breakage increased with confining pressure and consequently, the generalized shear stress ratio curve still declined to a certain degree after the peak stress is reached.

Fig. 6 shows the change curves in the generalized shear stress ratio (q/p) of the sample with axial strain (ε_1) in the consolidated undrained test.

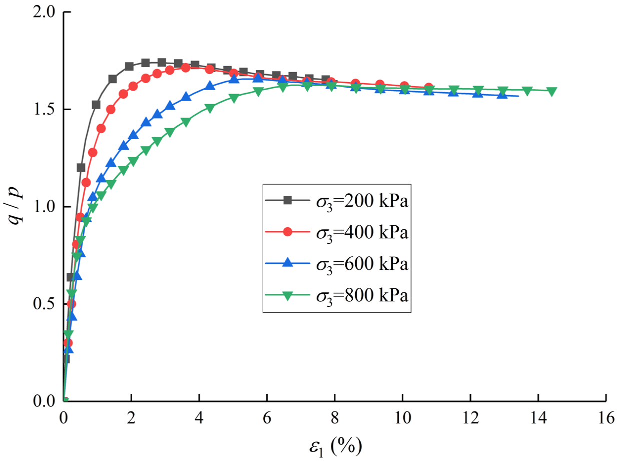

Fig. 6. Relation curves of shear stress ratio-axial strain of sample under undrained condition

As shown in the figure, the generalized shear stress ratio curves of the sample under undrained condition with confining pressures of 200 kPa, 400 kPa, and 600 kPa presented strain softening type with obvious peak values. For the sample under 800 kPa confining pressure, its generalized shear stress ratio curve presented continuous hardening type, which was identical with the low-pressure softening and high-pressure hardening laws of coarse-grained soil under general circumstances. In the initial phase, the curves presented linear growth trends and the initial slopes under four confining pressures were quite loose. Peak stress ratios of the curves declined as the confining pressure increased, but final generalized shear stresses were close. Fig. 11 shows that even though the grain breakage index of the sample increased with confining pressure in the consolidated undrained test, grain breakage remained small under high confining pressure and breakage rate was low, which had a minor effect on sample strength. Therefore, the curves presented hardening type under high confining pressure.

4.2 Deformation characteristic analysis

Fig. 7 shows the change curves of volumetric strain (ε_v) with axial strain (ε_1) of the sample in the consolidated drained test.

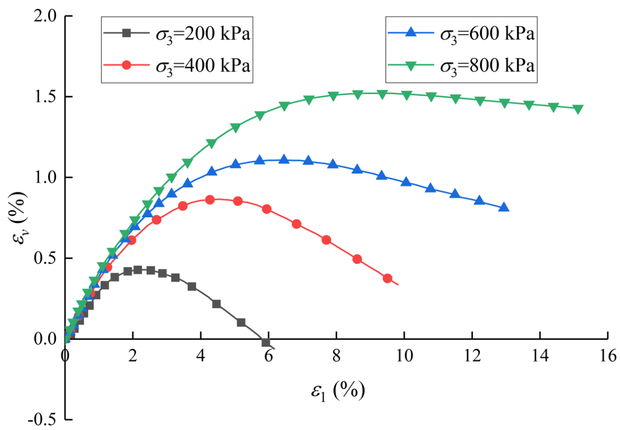

Fig. 7. Relation curves of volumetric strain-axial strain of the sample under drained condition

As shown in Fig. 7, the volumetric strains of the sample first increased and then decreased with axial strain under four confining pressures, thereby indicating that the sample first experienced shear shrinkage and then shear dilation. As the confining pressure increased, the shear shrinkage of the sample increased while shear dilation decreased. When the confining pressure was 800 kPa, the falling range of the volumetric strain curve was small, that is, the volumetric strain presented mainly shear shrinkage while shear dilation was not obvious.

In Fig. 7, the sample shear shrinkage increased continuously while the shear dilation declined gradually as the confining pressure increased, mainly because under the effect of confining pressure, the sample experienced compaction process until grain breakage. The sample was compacted continuously while shear shrinkage was enlarged continuously as the confining pressure increased. In the shear process, even though volume deformation continued to develop towards the direction of the shear dilation, the grain breakage gradually became serious as the confining pressure increased (Fig. 11), which inhibited the development of shear dilation, causing the shear dilation trend to become increasingly weaker. In the tri-axial shear test of calcareous sand, Zhang et al. [24] found that shear dilation under low confining pressure had a greater effect on material strength than grain breakage. The degree of material grain breakage became serious as the confining pressure increased and the effect of grain breakage on material strength became even more significant.

Fig. 8 shows the development curves of porewater pressure (u_w) with axial strain (ε_1) of the sample in the consolidated undrained test, where the porewater pressure was measured using a pore pressure sensor on the sample top and the measurements acquired automatically by a computer.

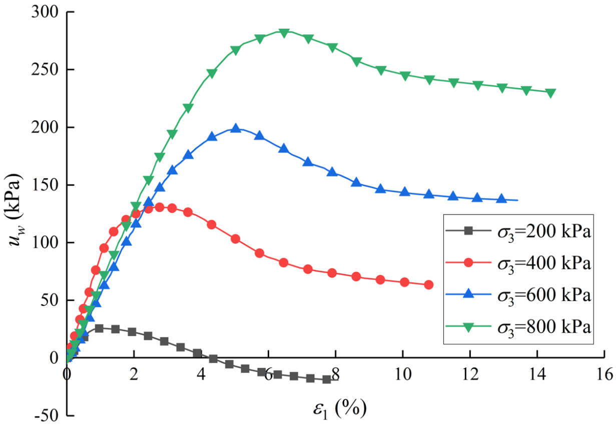

Fig. 8. Relation curves of pore water pressure-axial strain of sample under undrained condition

Fig. 8 shows that except for the sample under 200 kPa, porewater pressures of other samples had an abrupt increasing process and then slowly dissipated. As the confining pressure increased, peak porewater pressure increased continuously. For the sample under 200 kPa, its porewater pressure started declining gradually at an axial strain of 1% as the loading proceeded until it was reduced to a negative value. For samples under 400 kPa, 600 kPa, and 800 kPa, their porewater pressures started declining under axial strains of 3%, 5%, and 6%, respectively. In the consolidated undrained shear test, it is generally believed that sample volume would not change. However, in a study of shear dilation mechanism of sandy soil, Chi et al. [27] found that for samples with high stone content, sliding extrusion, breakage, and gap filling could be observed between rock blocks in the shear process and hence, shear dilation and shear shrinkage also occurred.

Pore pressure coefficient was used to characterize change trend of sample volume to explore the deformation laws of the sample under undrained conditions and is defined as follow:

$$A = \frac{u_w}{(\sigma_1 - \sigma_3)} \tag{1}$$

where $A > 0$ represents shear shrinkage while $A < 0$ means shear dilation. Fig. 9 gives the change graph of pore pressure coefficient with axial strain.

At the initial loading phase, pore pressure coefficients under four confining pressures could be observed to undergo first an increase then a decline to zero process, indicating that the sample went through volume shrinkage, but the volume shrinkage trend gradually became gentle. As the loading proceeded, pore pressure coefficient of the sample under 200 kPa confining pressure became 0 when axial strain reached 1% or so, and subsequently, pore pressure coefficient continued to decline to a negative value, indicating that the sample volume turned from shrinkage into dilation. For samples under 400 kPa, 600 kPa, and 800 kPa, their pore pressure coefficients became 0 when axial strain reached 3%, 5%, and 6%, respectively and then declined to negative values. Moreover, the sample volume went from shrinkage into dilation.

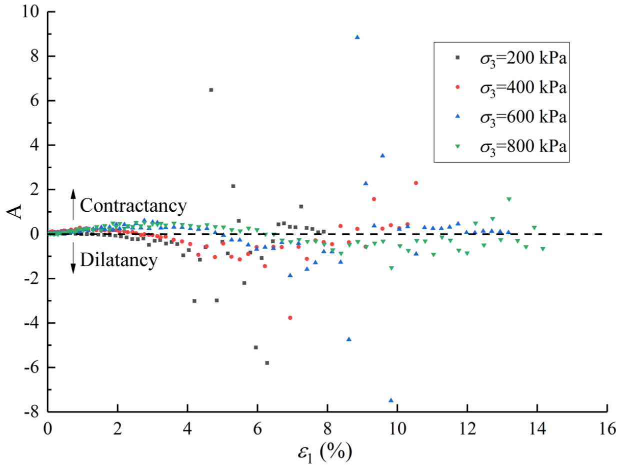

Fig. 9. Relationship between pore water pressure coefficient and axial strain

This finding corresponds to the change curve of porewater pressure, that is, the sample experienced shear shrinkage when porewater pressure increased and shear dilation when porewater pressure declined. Xia et al. [28] found similar laws when conducting a tri-axial undrained shear test of earth-rock aggregate. Porewater pressure started declining after increasing to peak value, the sample went from shear shrinkage into shear dilation, and the maximum value of the pore pressure coefficient basically corresponded to the peak rate of the porewater pressure curve. The point with pore pressure coefficient being 0 was the phase transformation point of sample volume change. Fig. 11 shows that the sample grain breakage was small under undrained condition. The sample presented shear dilation under 200 kPa confining pressure, which was caused by the grain position adjustment under low confining pressure. The confining pressure then increased and the sample compacted, causing grain breakage to occur as the loading proceeded. Notably, in the pore pressure coefficient distribution graph in this test, the discreteness of individual point was large, which could be attributed to the sudden changes in the position and morphology of large grains in the shear process. However, these changes did not affect the overall change trend of the sample volume.

4.3 Strength characteristic analysis

In the tri-axial compression path, the calculation formula of internal friction angle corresponding to any η is

$$\sin\varphi = \frac{3\eta}{6+\eta} \tag{2}$$

where φ is internal friction angle and η is the generalized shear stress ratio, $\eta = q / p$.

The peak friction angle and critical friction angle of the specimen can be calculated according to the maximum and final values of the generalized shear stress ratio curve using

Equation (2). For the hardening-type curve, the peak friction angle was made equal to the critical friction angle. Fig. 10 gives the change curves of the peak and the critical friction angles of the specimen with confining pressure in the consolidated drained and consolidated undrained shear tests. $\varphi_{p,cd}$ and $\varphi_{cs,cd}$ are the peak and the critical friction angles in the consolidated drained test, respectively. $\varphi_{p,cu}$ and $\varphi_{cs,cu}$ are respectively the peak and critical friction angles in the consolidated undrained test. According to Fig. 10, both peak friction angle and critical friction angle of the sample declined as the confining pressure increased in both the consolidated drained and consolidated undrained shear tests. Both the peak and the critical friction angle obtained through the consolidated drained test were larger than those obtained through the undrained test. Qin et al. [26] also obtained similar results for the tri-axial test for sericite schist.

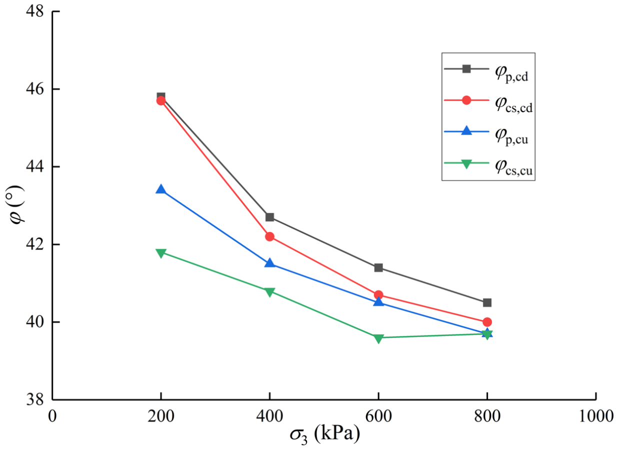

Fig. 10 Change curves of peak friction angle and critical friction angle with confining pressure

4.4 Effect of grain breakage on mechanical properties of coarse-grained fillers

Fig. 11 shows the relation curves between grain breakage index and confining pressure obtained through sample sieving in this test. Fig. 12 gives the relation curves of grain breakage index of coarse-grained filler with peak and critical friction angles.

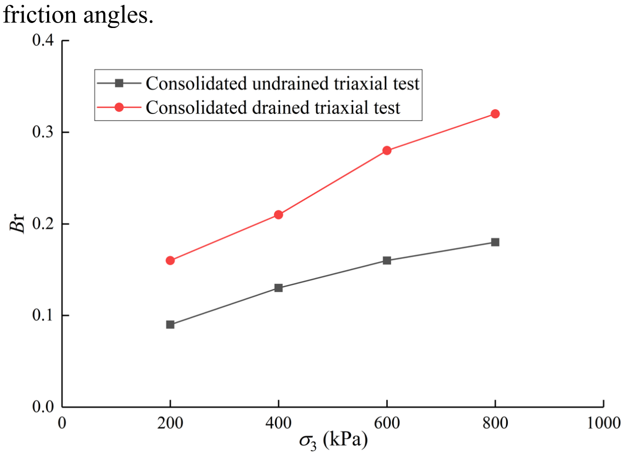

Fig. 11. Relation curves between grain breakage index and confining pressure

Fig. 12 shows that both peak and critical friction angles of the sample declined significantly with grain breakage index in the consolidated drained and consolidated undrained tests. Under undrained conditions, the critical friction angle of the sample under 800 kPa confining pressure increased incrementally. Many studies [23-24, 29] have found that increasing grain breakage has led to a reduction in the internal friction angle of the material.

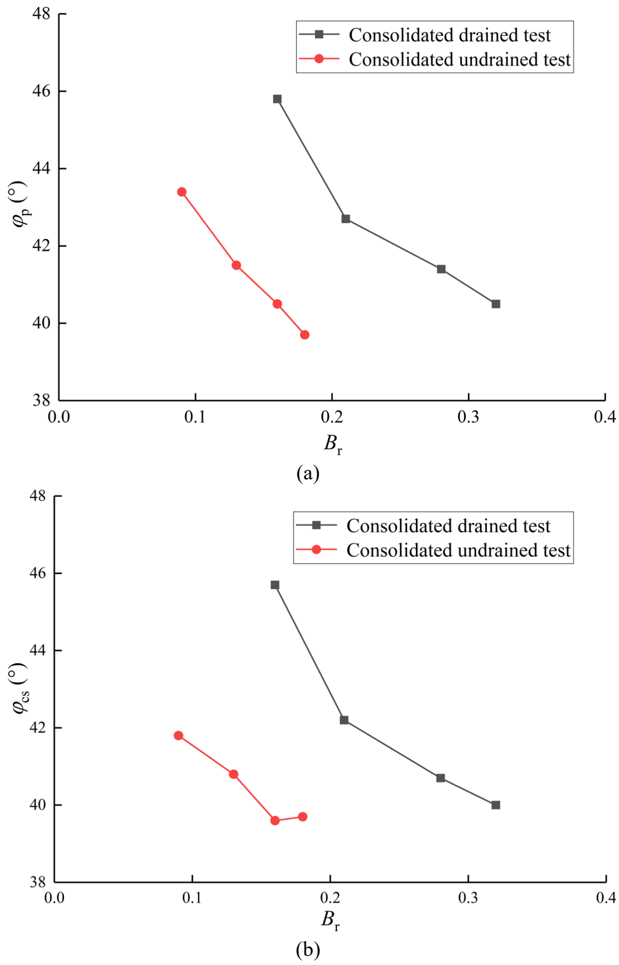

Fig. 12. Change curves of the peak and critical friction angles with grain breakage index

The sample under drained condition experienced weak strain softening and shear dilation trend weakening phenomena under high pressure. The sample under the undrained condition presented obvious strain hardening and shear dilation features under high pressure. Fig. 11 clearly shows that grain breakage increased continuously with confining pressure. Both grain breakage and breakage rate of the sample under the drained condition were larger than those under the undrained condition. Grain breakage gave rise to grain rearrangement in the sample and small grains gradually filled the pores inside the sample, which weakened the shear dilatancy and affected the peak strength of the coarse-grained fillers.

Fig. 12 shows that the decrements of the peak and critical friction angles of the specimen were large when the grain breakage index increased under the drained condition, while those under the undrained condition were relatively small. Miura et al. [30] investigated the deformation and strength characteristics of coarse-grained materials and found that grain breakage would weaken shear dilatancy of the soil mass, reduce peak internal friction angle and significantly impact shear strength of the soil mass.

5. Duncan-Chang model analysis

Tab. 2 gives the Duncan-Chang model parameters obtained through the consolidated drained test.

Table 2. Duncan-Chang model parameters

Test material	c (kPa)	φ(°)	K	n	R_f	G	F	D	K_b	m
Argillaceous limestone	94	38.2	1410.8	0.21	0.81	0.36	0.09	6.03	831.4	0.03

The volumetric strain of coarse-grained fillers under the triaxial compression path can be analyzed using tangential Poisson's ratio υ_t : when υ_t is greater than 0.5, the filler presents hear dilation, and the greater the υ_t value, the more obvious the shear dilation; when υ_t is smaller than 0.5, the filler presents shear shrinkage, and the shear shrinkage becomes more obvious as the υ_t value becomes smaller [31].

Fig. 13 shows relation curves between tangential Poisson's ratio υ_t and stress level S of embankment filler calculated using the $E \sim \mu$ and $E \sim B$ models. The figure indicates that the Poisson's ratios calculated through both models increased gradually with the stress level, both gradually increasing from smaller than 0.5 to greater than 0.5. However, the Poisson's ratio calculated through the $E \sim \mu$ model presented a sudden change under high stress level with high discreteness. The curve obtained through the $E \sim B$ model was smooth and as the stress level increased, the sample underwent a change from shear shrinkage into shear dilation. Shear shrinkage reduced while shear dilation increased as the confining pressure increased. However, this finding contradicts the laws as revealed by the volumetric strain curve (Fig. 7). A large number of test results indicate that coarse grains present shear dilation under low confining pressure and shear shrinkage under high confining pressure. Therefore, $E \sim B$ model cannot describe the volumetric strain characteristics of the filler very well.

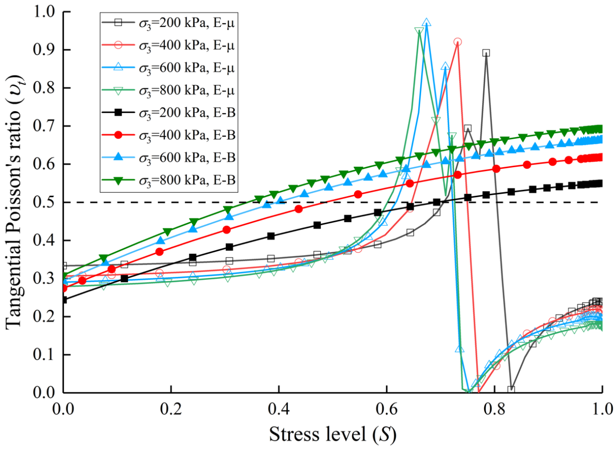

Fig. 13. Relation curves of the Poisson's ratio and stress level of the sample obtained through $E \sim \mu$ and $E \sim B$ models under different confining pressures

Fig. 14 shows the $\varepsilon_1 \sim \varepsilon_3$ curves of the sample under different confining pressures. Fig. 15 gives $\varepsilon_3 / \varepsilon_1 \sim \varepsilon_1$ curves under different confining pressures, which are fitted using a straight line.

The figure shows that $\varepsilon_1 \sim \varepsilon_3$ curves present hyperbolic relation under low confining pressure (200 kPa) but do not present an obvious hyperbolic relation under other confining pressures. The $\varepsilon_3 / \varepsilon_1 \sim \varepsilon_1$ curves have no obvious linear relations under four confining pressures, indicating that hyperbolic hypothesis between ε_1 and ε_3 is not applicable to this coarse-grained filler and that $E \sim \mu$ model cannot be used to describe accurately the deformation characteristics of this filler.

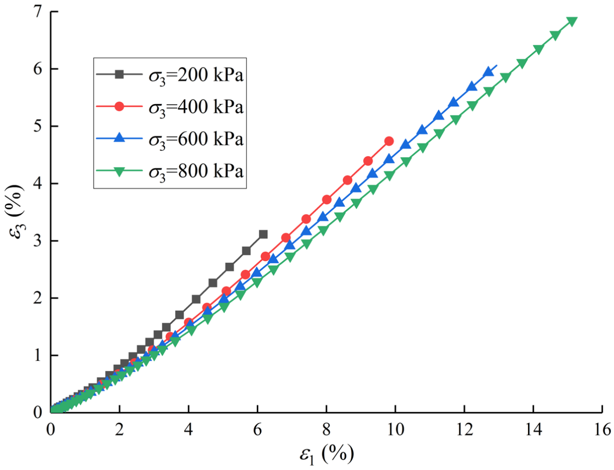

Fig. 14. $\varepsilon_1 \sim \varepsilon_3$ relation curves of the samples under different confining pressures

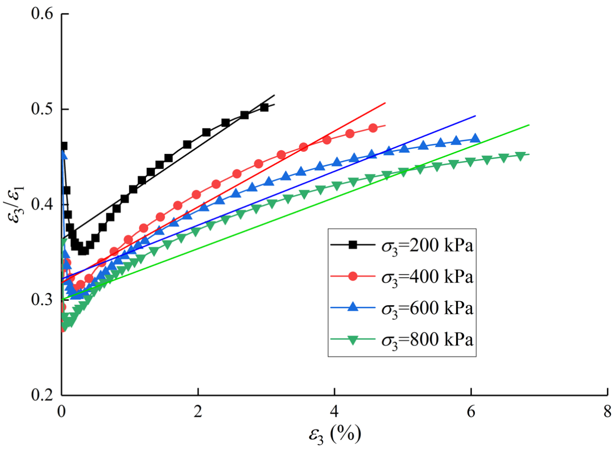

Fig. 15. $\varepsilon_3 / \varepsilon_1 \sim \varepsilon_1$ relation curves of the samples under different confining pressures

6. Conclusions

In this study, tri-axial consolidated drained and triaxial consolidated undrained shear tests were carried out to obtain a deeper understanding of the deformation characteristics of a coarse-grained high embankment filler. The stress-strain relation, deformation, and strength characteristics of coarse-grained argillaceous limestone fillers were analyzed and discussed, and the following conclusions were obtained:

In the triaxial shear test, strain softening phenomenon of coarse-grained soil occurs mostly under low confining pressure while strain hardening phenomenon appears under high confining pressure. The coarse-grained argillaceous limestone filler experiences strain softening phenomenon under high confining pressure in the consolidated drained shear test but presents low-pressure softening and high-pressure hardening in the consolidated undrained shear test. The main cause of these phenomena was found to be grain breakage, which causes changes in the sample grading and strength, consequently, strain softening appears in the high confining pressure phase under the drained condition.

Under drained and undrained conditions, coarse-grained argillaceous limestone filler first undergoes shear shrinkage and then shear dilation. However, in the consolidated drained test, its shear dilation trend is very weak under high pressure. The results indicate that grain breakage plays a dominant role in the sample deformation process because of its aggravation under high pressure which inhibits the development of shear dilation of the coarse-grained filler. In the consolidated undrained test, pore pressure coefficient is used to reflect the sample deformation characteristics. The results indicate that the change of pore pressure coefficient had a good corresponding relationship with the change of porewater pressure. Hence, the pore pressure coefficient can reflect intuitively the volumetric strain laws of coarse-grained soil under the undrained condition.

Changes in the peak and critical friction angles of coarse-grained argillaceous limestone filler obviously rely on stress path and are related closely to the grain breakage process. Both peak and critical friction angles obtained through the drained shear test are greater than those obtained through the undrained test. Under serious grain breakage, the peak and critical friction angles were reduced considerably with grain breakage index. If the grain breakage degree is light, the peak and critical friction angles are reduced lightly with grain breakage index.

Duncan-Chang model parameters are given on the test basis and model applicability is analyzed. Neither the $E \sim \mu$ nor the $E \sim B$ models in the Duncan-Chang model could describe accurately the deformation characteristics of embankment filler.

The study results can provide a certain test basis for analyzing the engineering mechanical characteristics of coarse-grained high embankment fillers and embankment stability, but the influence of grain breakage in the sample preparation process is not considered. Materials with different lithologies have different properties because of the diversity of engineering geology. Therefore, fillers with different lithologies and grades should be compared under complicated conditions in the future. The knowledge range of coarse-grained fillers should also be expanded by considering the multi-factor influence to provide a reference for a deeper understanding of the mechanical deformation properties of coarse-grained fillers.

Acknowledgements
This work was supported by the National Natural Science Foundation of China (Grant No. 51179106).

References

1. Guo, Q. G., "*Engineering properties and application of coarse-grained soil*". Zhengzhou: Yellow River Water Conservancy Press, China, 1998, pp.1-2.
2. Zhang, B., Qu, Z. J., "Stress-strain model of coarse-grained soil considering dilatancy and softening characteristics". *Chinese Journal of Geotechnical Engineering*, 13(6), 1991, pp.64-69.
3. Liao, H. J., Pu, W. C., Qing, W. C., "Study on softening constitutive model of diatomaceous soft rock based on strain space". *Rock and Soil Mechanics*, 27(11), 2006, pp.1861-1866.
4. Rowe, P. W., "The stress-dilatancy relation for static equilibrium of an assembly of grains in contact". *Proc Royal Society*, London, A269, 1962, pp.500-527.
5. Wan, R. G., Guo, R. G., "A simple constitutive model for granular soils: modified stress-dilatancy approach". *Computers and Geotechnics*, 22(2), 1998, pp.109-133.
6. Gajo, A., Wood, D. M., "Severn-Trent sand: a kinematic-hardening constitutive model: the q-p formulation". *Geotechnique*, 49(5), 1999, pp.595-614.
7. Lenart, S., Koseki, J., Miyashita, Y., Sato, T., "Large-scale triaxial tests of dense gravel material at low confining pressures". *Soils and Foundations*, 54(1), 2014, pp.45-55.
8. Zhu, J. G., Mohamed, A. A., Gong, X., Xuan, X. Y., Ji, E. Y., "Triaxial tests on wetting deformation behavior of a slate rockfill material". *Chinese Journal of Geotechnical Engineering*, 35(1), 2013, pp.170-174.
9. Liu, S. H., Shao, D. C., Shen, C. M., Wang, Z. J., "Microstructure-based elastoplastic constitutive model for coarse-grained materials". *Chinese Journal of Geotechnical Engineering*, 39(5), 2017, pp.777-783.
10. Zhao, N., Zuo, Y. Z., Wang, Z, B., Yu, S. G., "Grading scale method for coarse-grained soils based on fractal theory". *Rock and Soil Mechanics*, 37(12), 2016, pp.3513-3519.
11. Sun, Y. F., Liu, H. L., Yang, G., "Yielding function for coarse aggregates considering gradation evolution induced by grain breakage". *Rock and Soil Mechanics*, 34(12), 2013, pp.3479-3484.
12. Yang, G., Xu, J. B., Liu, K. L., "Numerical simulation of grain breakage of coarse aggregates". *Rock and Soil Mechanics*, 36(11), 2015, pp.3301-3306.
13. Khalkhali, B. A., Mirghasemi, A. A., "Numerical and experimental direct shear tests for coarse-grained soils". *Particuology*, 7, 2009, pp.83-91.
14. Jiang, J. S., Cheng, Z. L., Zuo, Y. Z., Ding, H. S., "Experimental investigation on strength behavior of coarse-grained materials under three-dimensional stress state". *Rock and Soil Mechanics*, 39(10), 2018, pp.1-8.
15. Tutumluer, E., Huang, H., Hashash, Y. M. A., Ghaboussi, J., "*Imaging based discrete element modeling of granular assemblies*". Melville: American Institute of Physics, American, 2008, pp.544-549, 973.
16. Bian, X. C., Li, G. Y., Li, W., Jiang, H. G., "Morphology analysis of coarse aggregate based on 3D imaging method by using two planar mirrors". *China Civil Engineering Journal*, 41(9), 2014, pp.135-144.
17. Dorostkar, O., Mirghasemi, A. A., "On the micromechanics of true triaxial test, insights from 3D DEM study". *Iranian Journal of Science and Technology-Transactions of Civil Engineering*, 42, 2018, pp.259-273.
18. Zhao, H. F., Zhang, L. M., "Bimodal shear-strength behavior of unsaturated coarse-grained soils". *Journal of Geotechnical and Geoenvironmental Engineering*, 139(12), 2013, pp.2070-2081.
19. Meng, F., Zhang, J. S., Chen, X. B., Wang, Q. Y., "Deformation characteristics of coarse-grained soil with various gradations". *Journal of Central South University*, 21, 2014, pp.2469-2476.
20. Shi, W. C., Zhu, J. G., Chiu, C. F., Liu, H. L., "Strength and deformation behavior of coarse-grained soil by true triaxial tests". *Journal of Central South University of Technology*, 17, 2010, pp.1095-1102.
21. Fu, W. X., Zheng, X., Lei X. Z., Deng J. H., "Using a modified direct shear apparatus to explore gap and size effects on shear resistance of coarse-grained soil". *Particuology*, 23, 2015, pp.82-89.
22. Hardin, B. O., "Crushing of soil grains". *Journal of Geotechnical Engineering, ASCE*, 111(10), 1985, pp.1177-1192.
23. Liu, H. L., Qin, H. Y., Gao, Y. F., Zhou, Y. D., "Experimental study on grain breakage of rockfill and coarse aggregates". *Rock and Soil Mechanics*, 26(4), 2005, pp.562-566.
24. Zhang, J, M., Jiang, G. S., Wang, R., "Research on influences of grain breakage and dilatancy on shear strength of calcareous sands". *Rock and Soil Mechanics*, 30(7), 2009, pp.2043-2048.
25. Jia, Y. F., Wang, B. S., Chi, S. C., "Grain breakage of rockfill during triaxial tests". *Chinese Journal of Geotechnical Engineering*, 37(9), 2015, pp.1692-1697.

26. Qin, S. L., Yang, L. Q., Gao, H., Chen, S. X., Luo, W. J., "Experimental study of mechanical properties of coarse aggregates of sericite schist under different stress paths". *Chinese Journal of Rock Mechanics and Engineering*, 33(9), 2014, pp.1932-1938.
27. Chi, M. J., Zhao, C. G., Li, X. J., "Stress-dilation mechanism of sands". *China Civil Engineering Journal*, 42(3), 2009, pp.99-104.
28. Xia, J. G., Hu, R. L., Qi, S. W., Gao, W., Sui H. Y., "Large-scale triaxial shear testing of soil rock mixtures containing oversized grains". *Chinese Journal of Rock Mechanics and Engineering*, 36(8), 2017, pp.2031-2039.
29. Liu, M. C., Gao, Y. F., Liu, H. L., "Effect of grain breakage on strength and deformation of modeled rockfills". *Chinese Journal of Geotechnical Engineering*, 33(11), 2011, pp.1691-1699.
30. Miura, N., Ohara, S., "Grain crushing of a decomposed granite soil under shear stresses". *Soils and Foundations*, 19(3), 1979, pp.61-76.
31. Zhang, G., Zhang, J. M., "Study on behavior of coarse-grained soil and its modeling". *Rock and Soil Mechanics*, 25(10), 2004, pp.1587-1591.